Available online at www.sciencedirect.com
ScienceDirect
Journal of Catalysis 252 (2007) 11–17
JOURNAL OF CATALYSIS
www.elsevier.com/locate/jcat

Methane oxidation over alumina supported platinum investigated by time-resolved *in situ* XANES spectroscopy

Elin Becker [a,b,*], Per-Anders Carlsson [a,b], Henrik Grönbeck [a,c], Magnus Skoglundh [a,b]

[a] *Competence Centre for Catalysis, Chalmers University of Technology, SE-412 96 Göteborg, Sweden*
[b] *Department of Chemical and Biological Engineering, Chalmers University of Technology, SE-412 96 Göteborg, Sweden*
[c] *Department of Applied Physics, Chalmers University of Technology, SE-412 96 Göteborg, Sweden*

Received 5 June 2007; revised 24 August 2007; accepted 12 September 2007

Available online 10 October 2007

Abstract

In situ time-resolved X-ray absorption spectroscopy and mass spectrometry were used to correlate changes in catalyst surface composition with catalytic activity for methane oxidation over alumina supported Pt. Different transient experiments (i.e., pulsing of oxygen or hydrogen to an otherwise constant gas composition) were performed to study the methane oxidation kinetics. Changes in the surface O/Pt ratio were monitored by the introduction of a new analysis method of the white line area corresponding to the Pt L_{III}-edge XANES spectra. The relevance of the method was confirmed by first-principles calculations demonstrating how hydrogen and oxygen adsorbates modify the electronic structure of Pt. The experimental results show that during the gas-phase transients, the surface O/Pt ratio changes, which in turn affects the methane oxidation rate. Activity maxima are observed for an intermediate surface O/Pt ratio. An oxygen-rich surface seems to hinder the dissociative adsorption of methane, leading to low methane oxidation activity at oxygen excess.

Keywords: Heterogeneous catalysis; Transient methods; X-ray absorption spectroscopy; Dissociative adsorption; Platinum oxide; CH_4; Pt; Pt/Al_2O_3

1. Introduction

The growing concern about global warming has stimulated strategies to reduce anthropogenic emissions of greenhouse gasses like carbon dioxide (CO_2). One such initiative within the transportation sector is to replace vehicles with gasoline or diesel engines with natural gas vehicles (NGVs). Since natural gas essentially is methane (CH_4), NGVs may reduce CO_2 emissions if the used methane is produced from regenerable sources, e.g., biomass. Moreover, NGVs have other advantages, such as low particulate and NO_x emissions as compared with, for example, standard diesel vehicles. But because CH_4 is also a significant greenhouse gas [1], the methane slip from the combustion process must be controlled, preferably by efficient catalytic exhaust aftertreatment systems. The rather cold exhaust (<500 °C) from these engines demands low-temperature active catalysts.

The most common catalysts for methane oxidation are Pd and Pt. Palladium is more active in the oxidised state and consequently is preferred for operation at net-oxidizing (lean) conditions, whereas Pt, which is more active in the metallic state, may be beneficial for net-reducing (rich) conditions [2–4]. Among the hydrocarbons, methane is the most difficult to oxidize, as reflected by the relatively high temperatures required for the catalytic oxidation to proceed. From a mechanistic standpoint, the low reactivity of methane is connected to the difficulty in which adsorption occurs on different catalytic surfaces. For example, the sticking probability of methane on noble metals is relatively low compared with that on higher alkanes [5]. This indicates that properties like the chemical state and morphology of the surfaces, which are crucial for the adsorption, are important for the overall oxidation rate. For example, it has been shown that the methane conversion over a Pt/Al_2O_3 catalyst strongly depends on the oxidizing–reducing character of the exhausts, in which excess oxygen conditions result in low

* Corresponding author.
E-mail address: elinb@chalmers.se (E. Becker).

0021-9517/$ – see front matter
doi:10.1016/j.jcat.2007.09.004

activity [6]. The latter was assumed to be due to deactivation of the Pt crystallites by adsorbed oxygen, decreasing the ability of the catalyst surface to dissociate methane.

X-ray absorption spectroscopy (XAS) is a powerful technique for analysis of, for example, the oxidation state of solids, and thus is used in many fields of research, including chemical sensors, semiconductors, and catalysts [7]. In an XAS spectrum, the extended X-ray absorption fine structure (EXAFS) region provides information on the local geometry and neighboring atoms of the absorbing atom [8]. The EXAFS spectra are sensitive to thermal vibrations and may degrade significantly at temperatures above 300 °C [9], that is, slightly below typical reaction temperatures for oxidation of saturated hydrocarbons over noble metals. But at these temperatures, it is still possible to deduce valuable information from XAS by using the region close to the absorption edge, the so called X-ray absorption near-edge structure (XANES) region. The XANES spectra provide information about the electronic structure of the absorbing atom and thus can reveal information about the chemical state of catalyst surfaces. For example, XANES has been used to study hydrogen [10–12] and CO chemisorption [12], as well as the influence of support material on the chemical state of Pt for typical supported catalysts [13]. The intensity of the absorption edge, the so-called white line [14], is connected to electron transitions from the atomic $2p_{3/2}$ state to the $5d_{3/2}$ and $5d_{5/2}$ levels. An intense white line is observed if the absorbing atom has a large number of d-electron vacancies. Consequently, the white line can be correlated to the oxidation state of platinum as the electron vacancies in the 5d levels reflect the oxidation state of the metal. For oxidized platinum, an intense white line is observed, as opposed to metallic platinum, where the white line is significantly less intense. Different methods based on the height and/or area of the white line have been used to extract quantitative information from XANES measurements [15]. Somewhat more sophisticated methods involving mathematical analysis of the area under the white line by fitting an arc tangent and a Gaussian or Lorentzian function to the spectra also have been used [16,17]. We previously reported the use of the energy difference at the inflection point of the absorption edge as a basis for analysis [18].

In the present study, we introduce a new method that uses the Pt L_{III} white line area (WLA) intensity to facilitate efficient evaluation of time-resolved *in situ* XANES measurements of methane oxidation over a Pt/Al_2O_3 catalyst at transient inlet conditions. Specifically, we correlate changes in the surface O/Pt ratio to methane oxidation activity during oxygen or hydrogen pulsing. To support the interpretation of the results that the method yields, we perform a set of first-principles calculations to study changes of the metal electronic density of states on O and H chemisorption.

2. Experimental

2.1. Catalyst preparation and characterization

A 4% Pt/Al_2O_3 catalyst was prepared by wet impregnation. The support material, 3.8 g γ-Al_2O_3 (SCC a-150/200, Sasol), was dispersed in 10 g of distilled water, and the pH was adjusted to 2.5 by adding diluted HNO_3 solution (Merck). An aqueous platinum nitrate solution ($Pt(NO_3)_2$, 0.15 wt%, Johnson Matthey) was added dropwise to the alumina slurry under continuous stirring to yield a Pt loading of 4%. The slurry was kept under continuous stirring for 20 min, frozen with liquid nitrogen, and freeze dried. To preserve a high Pt dispersion, the catalyst was calcined at 450 °C for 4 h in air, starting with a temperature ramp from room temperature at a rate of 5 °C per minute to 450 °C. The platinum dispersion of the final catalyst was determined by CO chemisorption (Micromeritics, ASAP2010C) at 27 °C, giving 65% dispersion assuming a maximum CO/Pt ratio of 0.8, which is reasonable for highly dispersed Pt particles [19]. The BET surface area (Micromeritics Tristar) of the sample was measured as 182 m^2/g.

2.2. In situ *XANES measurements*

Energy-dispersive *in situ* XANES measurements at the Pt L_{III}-edge (11.6 keV) were performed in transmission mode at beamline ID24 at ESRF, Grenoble, France, on a pressed pellet ($\varnothing = 5.3$ mm and $l = 1.3$ mm) of ca 50 mg 4% Pt/Al_2O_3 and 50 mg KBr. The x-ray beam spot size on the sample was $\sim 200 \times 200$ μm, and the data sampling rate was 0.56 s. The pellets were mounted in a temperature-controlled flow reactor cell, to which a reactant gas mixture, obtained through individual mass flow controllers, was introduced. A total flow of 100 ml/(NTP)min, corresponding to a space velocity of about 70,000 h^{-1}, was used. The reactor cell was mainly a flow-by type with a volume of ∼5 ml, here resulting in a residence time of <3 s. The product stream was continuously analyzed with a Balzers Prisma mass spectrometer following the H_2 (m/e 2), He (m/e 4), CH_3 (m/e 15), H_2O (m/e 18), CO (m/e 28), O_2 (m/e 32), Ar (m/e 40), and CO_2 (m/e 44) signals. The beamline was equipped with a Si [111] polychromator crystal, operating in Bragg mode, for selection of the desired range of X-ray wavelengths (11.43–12.05 keV), and a 1152×1242 pixel CCD solid-state detector for spectral analysis. Two additional mirrors in the beamline were used to achieve harmonic rejection. The estimated energy resolution was $\Delta E/E \approx 1.2$–1.5×10^{-4}, and the energy increment between data points was 1.2 eV. The XANES spectra were recorded during pulse response (PR) experiments while the oxidising-reducing character of the feed was periodically varied by changing either the oxygen concentration between 0 (5 min) and 1250 vol-ppm (5 min) using a 500 vol-ppm CH_4 flow or a H_2 concentration between 0 (5 min) and 5000 vol-ppm (5 min) using a flow of 500 vol-ppm CH_4 and 1250 vol-ppm O_2. Helium was used as carrier gas in all experiments. The PR experiments were repeated at 450, 400, and 350 °C. All of the experiments are summarized in Table 1 together with the stoichiometric number, S, which is used to describe the oxidizing–reducing characteristics of the feed gas.

2.3. Method for evaluation of XANES spectra

Previously, the WLA was evaluated by fitting an arc tangent and Gaussian or Lorentzian function to the peak and then

Table 1
Summary of the PR experiments performed during the XANES measurements

Experiment	CH_4 conc. (ppm)	O_2 conc. (ppm)	H_2 conc. (ppm)	He conc.	S[a]
PR-O_2					
Lean	500	1250	–	Bal.	1.25
Rich	500	–	–	Bal.	0
PR-H_2					
Lean	500	1250	0	Bal.	1.25
Rich	500	1250	5000	Bal.	0.36

[a] $S = 2[O_2]/([H_2] + 4[CH_4])$ [43].

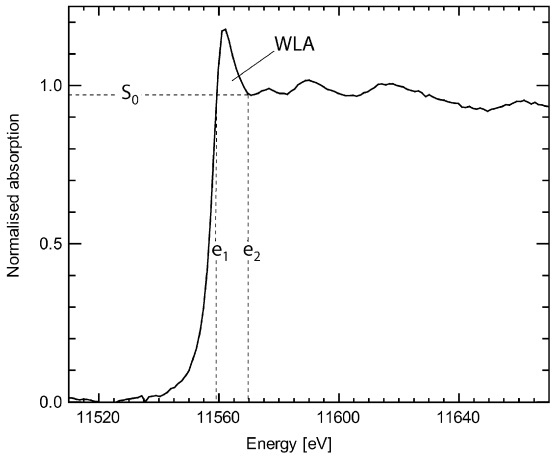

Fig. 1. XANES Pt L_{III}-edge spectra recorded during exposure to 0.5% hydrogen, 1250 ppm O_2, 500 ppm CH_4. The WLA is calculated by selecting the first minimum of absorption after the edge, S_0, at energy e_2 as a starting point. The WLA is thereafter calculated as $\int_{e_1}^{e_2}(S(\varepsilon) - S_0)\,d\varepsilon$, where $S(\varepsilon)$ is the absorption spectrum and e_1 is the start of integration.

obtaining the WLA by integrating the function [20]. Such a procedure is suitable for analyzing relatively few spectra with large relative differences in WLAs. However, for the present set of data that contains thousands of spectra, such methods are not feasible and may not be able to capture small changes in the spectra. For that reason, we introduce a new analysis method facilitating evaluation of small changes in XANES spectra.

The time-resolved Pt L_{III} edge XANES spectra were initially energy-calibrated, using the Delia program in the XAID toolbox in the XOP 2.0 software package [21], by fitting the experimental data of a Pt foil spectrum to a corresponding spectrum measured in a non-energy-dispersive mode from the database DABAX. All spectra were then normalized, and the WLA of each spectrum was calculated by interpolation and integration. The WLA was calculated by selecting the first minimum of absorption after the edge, S_0, at energy e_2 as a starting point, $\int_{e_1}^{e_2}(S(\varepsilon) - S_0)d\varepsilon$, where $S(\varepsilon)$ is the absorption spectrum and e_1 is the start of integration, cf. Fig. 1. The present method has the advantage of being less sensitive to normalization of the spectra. Extracting quantitative information about the Pt oxidation state by using the WLA, as performed by Yoshida et al. [17], requires reliable reference spectra of samples with known oxidation states [i.e., Pt foil, Pt(II) oxide, and Pt(IV) oxide] obtained from the same experimental setup as the actual measurements. Unfortunately, because we have measurements only for the Pt foil, we cannot unambiguously perform a complete quantification of the oxidation state. But to extract as much information as possible, we instead used a reference spectrum from the DABAX database to obtain a value for the WLA of PtO_2. By using this value and the value for the Pt foil as references, it is possible to correlate changes in the WLA to changes in the surface O/Pt ratio during reaction.

2.4. Computational method

To analyze how the electronic structure of a platinum surface is modified by adsorption of oxygen and hydrogen, we performed a set of first-principles calculations on the basis of the density functional theory (DFT) [22,23]. We used DFT in the implementation with plane waves and pseudopotentials [24]. In particular, we used the Perdew–Burke–Ernzerhof (PBE) approximation to the exchange and correlation functional [25], along with ultrasoft scalar relativistic pseudopotentials to describe the interaction between the valence electrons and the core [26]. A kinetic energy cutoff of 27.5 Ry was used to expand the Kohn–Sham orbitals. Reciprocal space integration over the Brillouin zone was approximated by (5,5,1) finite sampling using the Monkhorst–Pack scheme [27,28].

Using the present method, we calculated the lattice constant for Pt to be 4.00 Å. This is a slight overestimation compared with the experimental value of 3.92 Å [29]. Adsorption of oxygen and hydrogen was considered on a Pt(111) surface modeled by a p(2 × 2) unit cell with four atomic layers. In the calculations, repeated slabs were separated by 12 Å. To mimic a truncated bulk surface, the atomic positions for the bottommost layer were fixed at values corresponding to the theoretical bulk value. All other atoms in the cell were geometry-optimized.

3. Results

3.1. Experimental results

Fig. 2 shows the WLA of the Pt L_{III} edge *in situ* XANES spectra and the simultaneously recorded mass spectrometry data for the Pt/Al_2O_3 sample during an oxygen PR experiment at 400 °C. At the beginning of an oxygen step (e.g., $t = 10$ min), the outlet concentration of CH_4 decreased rapidly, reaching a minimum at about 7 s after the introduction of oxygen before the start of a continuous increase for the remaining period with oxygen supply. Most often, the methane concentration approaches a stationary level, however, in this case, the pulse time was too short to allow this observation. A corresponding increase in the amount of CO_2 produced, a transition through a concentration maximum, and a continuous decrease occurred for the same period. When the oxygen supply was switched off at $t = 15$ min, the CH_4 concentration passed a new minimum before approaching a significantly lower level compared with the period of oxygen supply. Considering the CO_2 concentration for this 5-min period, a corresponding passage through a concentration maximum before it reaches 50 ppm can be seen.

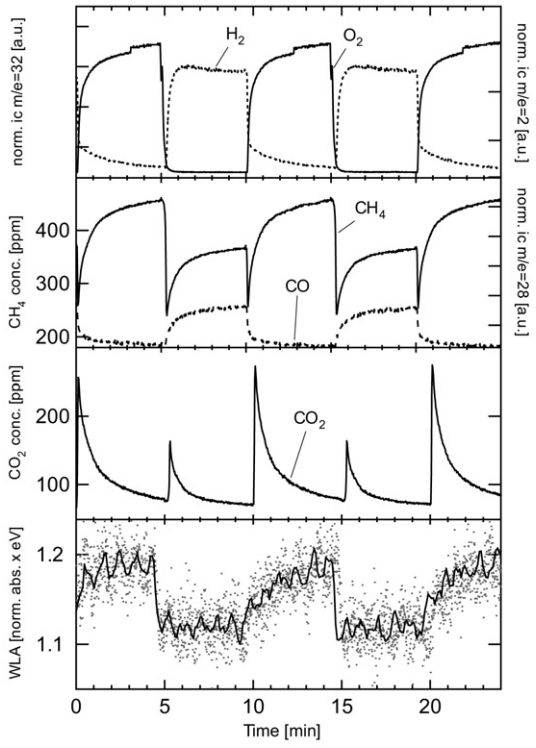

Fig. 2. Oxidation of 500 ppm CH_4 over a 4% Pt/Al_2O_3 catalyst at 400 °C during periodic changes of the oxygen concentration between 0 and 1250 ppm. From top to bottom: Normalised ion currents for H_2 (m/e 2) and O_2 (m/e 32), CH_4 concentration and normalised ion current for CO (m/e 28), CO_2 concentration and white line areas of the XANES Pt L_{III} edge spectra. The floating median of the WLA is represented by the black line in the bottom panel.

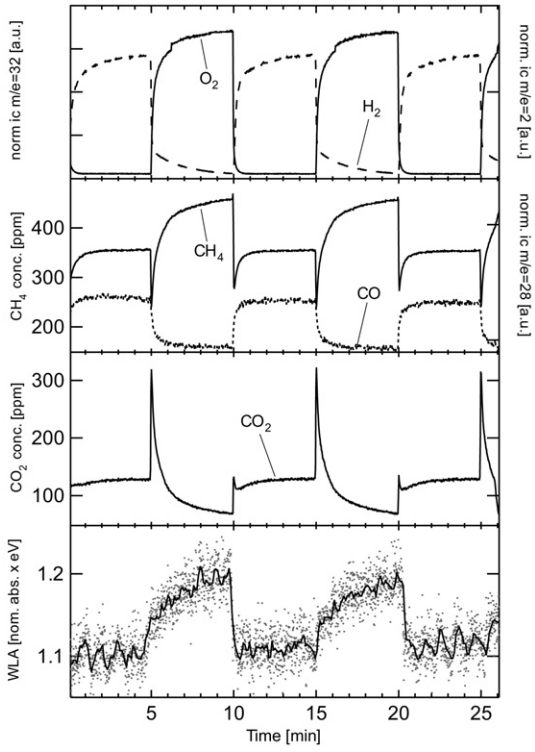

Fig. 3. Methane oxidation over a 4% Pt/Al_2O_3 catalyst at 400 °C during hydrogen pulsing (0.5%, 5 min) to a 500 ppm CH_4 and 1250 ppm O_2 composition. From top to bottom: Normalised ion currents for H_2 (m/e 2) and O_2 (m/e 32), CH_4 concentration and normalised ion current for CO (m/e 28), CO_2 concentration and white line areas of the XANES Pt L_{III} edge spectra. The floating median of the WLA is represented by the black line in the bottom panel.

During the rich phase (no oxygen supply), both carbon monoxide and hydrogen were produced. Considering the WLA for Pt during the pulses, the introduction of oxygen led to a continuously increasing WLA value, whereas a step decrease in the WLA occurred when the oxygen supply was switched off. The increase in WLA was relatively slow when the oxygen supply was switched on. When the oxygen was removed from the gas feed, the decrease in WLA was considerably faster. This trend was observed at all of the temperatures studied, and no clear temperature dependence could be observed. The periodic fluctuations in WLA shown in Fig. 2 were probably due to the combined effects of fluctuations of the X-ray beam position and sample inhomogeneities [30,31].

Fig. 3 shows the results from the PR experiment in which H_2 pulses (0.5%, 5 min) were introduced to a net-oxidizing mixture of CH_4/O_2/He at 400 °C. These results are in line with the oxygen PR experiments, with a relatively high outlet concentration of CH_4 in absence of hydrogen in the feed. However, introducing H_2 resulted in a sharp drop in the CH_4 concentration passing through a minimum, followed by a slow increase. When the H_2 supply was switched off at $t = 15$ min, there was a lower minimum correlated with an increase in the CO_2 concentration. Studying the changes in the WLA reveals a rather rapid drop in WLA with the introduction of hydrogen, followed by a slower increase when the hydrogen supply was switched off. No significant rate differences in WLA increase or decrease were found at the temperatures studied.

3.2. Computational results

To exemplify how adsorbates can modify the electronic structure of platinum, we performed first-principles calculations. We compared the electronic density of states (EDOS) of a bare Pt(111) surface with the case with O and H adsorbed on Pt(111). Fig. 4 shows the results corresponding to an adsorbate coverage of 0.25 monolayer. For O as well as H, the preferred adsorption site was the threefold fcc position.

Because the WLA reflects the number of unoccupied d-states, we projected the Kohn–Sham orbitals on the (pseudo) atomic orbitals of each atom. In the cases with adsorbates, the EDOS corresponding to a metal atom is one of the atoms forming the threefold site at which the adsorbates are chemisorbed.

The results clearly show the difference between oxygen and hydrogen adsorption on the electronic structure of the metal surface. Compared with oxygen, the changes induced by hydrogen were smaller. Because the EDOS of unoccupied states above the Fermi energy (ε_F) is of special interest, we integrated this part from ε_F to $\varepsilon_F + 5$ eV. For Pt(111), H/Pt(111), and O/Pt(111), we calculated 1.04, 0.94 and 1.17 electrons, respectively. Because the electronic configuration of platinum is $5d^9 6s^1$, the result for the bare surface (one electron hole in the d-shell) was as expected and confirmed the accuracy of the applied technique. Hydrogen was found to donate a fraction of one electron to the metal. For oxygen, the trend was reversed.

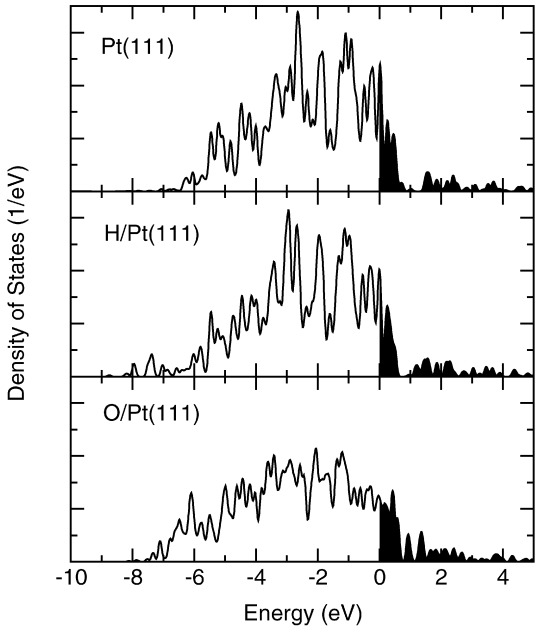

Fig. 4. Projected electronic density of states of Pt(111), H/Pt(111) and O/Pt(111). The results are reported with respect to the Fermi energy of each system and broaded with a 0.05-eV Gaussian. The shaded curves correspond to unoccupied states.

Oxygen abstracted an electronic charge from the metal, resulting in an increase in the d-electron vacancies. For completely oxidized Pt (PtO_2), there was an even higher degree of charge transfer from the metal, and the integrated EDOS for α-PtO_2 was 1.9 electrons.

4. Discussion

As mentioned in the Introduction, the electronic state of a solid catalyst surface is crucial to the catalytic activity. For Pt-based catalysts, this was demonstrated for many reactions, including oxidation of CO [18,32], C_3H_8 [33,34], and CH_4 [4,6]. The common result in these studies is that the degree of oxidation of the platinum surface has a significant impact on the overall reaction rate. Various terms, such as "weak" and "strong" adsorption of oxygen [35], or any version of surface oxide [36], have been used to describe various degrees of interaction between platinum and oxygen. These terms are often cited interchangeably in the literature. Following the definition of IUPAC, no clear distinction can be made between adsorbed oxygen and surface oxides [37]. Charge transfer adsorption is a form of reductive or oxidative adsorption in which reductive and oxidative refer to electron gain and loss, respectively, on species in the solid [37]. This is demonstrated by our DFT calculations that clearly show that hydrogen and oxygen adsorbed on Pt(111) affect the EDOS above the Fermi level, which in turn influences the electron density and thus also the number of unoccupied d-states. Oxygen adsorbed on Pt(111) gives an increased number of unoccupied d-states, which in a XANES spectrum gives rise to an increased white line intensity, whereas hydrogen adsorbed to Pt(111) results in a decrease of unoccupied d-states and thus a decrease in white line intensity. Thus, in the present study, we can confidently interpret an increase in the XANES WLA in terms of increased surface O/Pt ratio and vice versa. The term surface O/Pt ratio here considers the amount of oxygen in all types of platinum–oxygen species. This is because we cannot unambiguously distinguish between chemisorbed oxygen on the Pt crystallites and Pt oxide, because both types affect the surface electronic state, and the absolute quantification of the WLA is not straightforward. With the present interpretation of changes in the WLA, we then correlate the surface O/Pt ratio to the activity for methane oxidation and speculate as to how this may influence the dissociative adsorption of methane. In addition, we have some comments on the reaction selectivity.

In the oxygen PR experiment (cf. Fig. 2), we observed minima and maxima in the CH_4 and CO_2 outlet concentrations for changes from rich to lean (RL) and from lean to rich (LR) conditions. The high CO_2 production at the RL switch was most likely due to a combined effect of the passage through a state with high activity for some intermediate surface O/Pt ratio and high availability of adsorbed CH_x (methane adsorbs dissociatively on noble metals [2], however, the exact adsorbate configuration is not well understood) that has been accumulated during the oxygen-free period. The transient oxygen concentration on the catalyst surface is evident from the XANES analysis, which shows an increasing WLA for this period. The high methane oxidation activity at the switch is in line with previous studies on methane oxidation [6], and thus our XANES analysis confirms previous speculations that the surface O/Pt ratio plays an important role in the activity of this reaction.

The influence of the surface O/Pt ratio on activity is even more clear during the LR switch. Here the CH_x coverage is initially low; however, despite this, the activity is temporarily high which again is due to the transition through a state with high activity. It is likely that an optimal surface O/Pt ratio corresponding to a maximum methane oxidation rate exists. This is supported by the hydrogen PR experiments (cf. Fig. 3), which show similar results. In this case, a small overshoot in CO_2 production is observed during the initial period of H_2 supply. Even though the underlying mechanisms are different in the oxygen and hydrogen pulse experiments, we can see clear connections between surface O/Pt ratio and methane oxidation activity. Moreover, the XANES experiments indicate that at the conditions used here, the reduction process is faster than the oxidation process.

In this study, we used a Pt catalyst with 65% dispersion, meaning that most of the Pt atoms are available for adsorption. Here, this facilitates the detection of changes in WLA as a result of changes in the surface coverage. It was previously shown that Pt crystallite size distribution has a negligible influence on the XANES spectra [38]; thus, in our study, changes in WLA are relevant as a measure of changes in the surface O/Pt ratio. A comparison between the WLAs of the sample used in the present study and the reference samples (Pt foil and PtO_2) suggests that the average oxidation state of platinum is closer to zero (Pt) than +4 (PtO_2). Given that a linear relationship between the WLA and the O/Pt ratio is plausible [17], and using the WLA of Pt(0) = 0.95 and WLA of Pt(IV) = 5.87, we

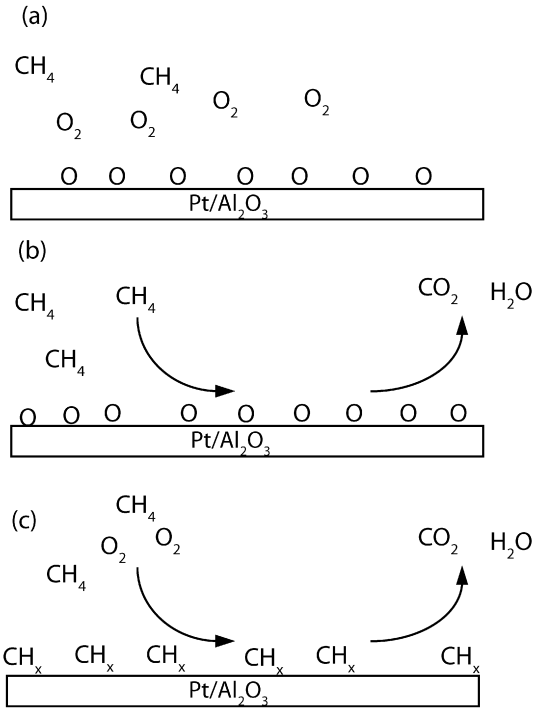

Fig. 5. Schematic illustration of possible mechanisms for dissociative adsorption of CH_4 on a catalyst surface for (a) an oxygen covered surface with a lean feed gas, (b) on a partially oxygen covered surface with only methane in the feed gas and (c) on an initially CH_x covered surface when oxygen is added to the methane feed gas.

may speculate that, assuming that the WLA during O_2 exposure (cf. Fig. 2) equals about 1.2, and assuming oxidation of surface Pt only, the average O/Pt ratio would be 0.16 for our sample. During the oxygen-free periods, WLA equals about 1.1; in this case, the corresponding average O/Pt ratio of the surface Pt would be 0.10. Thus, the O/Pt ratio is higher at the end of an O_2 pulse compared with at the end of an oxygen-free period by a factor of 1.6. The present results are in line with the study by Burch et al. [4], who measured the oxygen uptake of a reduced Pt/Al_2O_3 catalyst in vacuum at 300 °C and found that it (O/Pt) reached a stationary value of about 65% of a monolayer. This was correlated with the conversion of methane over the same catalyst, and it was found that maximum CH_4 conversion was reached just before the oxygen uptake reached 65%, after which the activity declined quite rapidly.

Considering the sticking probabilities of methane and oxygen together with the results from the PR experiments, the following scenario emerges (Fig. 5): In the presence of excess oxygen, the surface becomes increasingly covered with oxygen. This is supported by the fact that the sticking coefficient for oxygen is about 15 times higher than that for methane on Pt (although the sticking coefficient can vary depending on surface structure and experimental conditions) [39–42]. As a result, a relatively low amount of methane adsorbs on the Pt crystallites (which most likely is required for the catalytic reaction, assuming a Langmuir–Hinshelwood reaction mechanism), reflecting the low conversion at the end of an oxygen step (Figs. 5a and 2 at $t = 4$ min). Moreover, when the oxygen supply is switched off (Figs. 5b and 2 at $t = 5$ min), an increase in activity is observed. The activity increase is likely due to the removal of gas-phase oxygen, which competes with methane for the vacant adsorption sites on the Pt crystallites, thus leading to a change in surface O/Pt ratio favoring methane adsorption. When the catalyst is exposed only to methane (we assume the catalyst surface is covered with dissociated methane, which we denote by CH_x) and the oxygen supply is switched on (Fig. 5c and $t = 10$ min in Fig. 2), temporary high methane conversion is likely obtained until all CH_x is consumed.

During the rich period in both the oxygen and hydrogen PR experiments, CO_2 production decreases after the initial activity increase. The outlet methane concentration is lower than during the lean phase, and both H_2 and CO are produced. This indicates that methane adsorbs on the catalyst surface, and also that some of the methane is converted into CO and H_2. But this requires an oxygen source, which could be the remaining water produced in the previous oxidation reaction, oxygen from platinum oxide, or oxygen from carbonates on the support. Supposing that the Pt crystallites are oxidized during the lean phase and then reduced by CH_4 during the rich phase, this could produce some CO and H_2. But this is not probable given that the CO production increases during the oxygen-free phase and the WLA drops quite rapidly, indicating a relatively rapid reduction. Because the WLA remains at a fairly constant level during the oxygen-free period, the interpretation of the WLA clearly shows that the oxygen is not provided from the Pt surface region. Therefore, a more likely explanation is a reverse-methanation reaction, that is, water reacting with CH_4 to form H_2 and CO. Further possibilities are reactions of methane with hydroxyl species and/or carbonates from the support, where the reaction with hydroxyl species seems more probable, because the carbonates are likely rather unstable at the temperatures used in this investigation.

In summary, we have shown that the surface O/Pt ratio is crucial for methane oxidation activity. By performing transient experiments, we observed activity maxima for both LR and RL switches. This suggests that it is possible to approach an optimal surface O/Pt ratio for maximum methane oxidation by means of periodic operation of the gas phase, as was previously observed for oxidation of propane [33].

5. Conclusion

We have investigated methane oxidation over a Pt/Al_2O_3 catalyst *in situ* by combined XANES spectroscopy and mass spectrometry under transient reaction conditions. By introducing an analytical method that enables use of the WLA of the Pt L_{III}-edge XANES spectra, we were able to continuously follow small changes of the surface O/Pt ratio. To confirm the relevance of this method, we performed first-principles calculations to exemplify how hydrogen and oxygen adsorbates may modify the electronic structure of Pt. Based on this method, we correlated changes in surface O/Pt ratio to changes in methane oxidation activity. In particular, we could correlate the activity maxima observed at the switches during lean–rich cycling with an intermediate surface O/Pt ratio. For a rich–lean switch, the activity maximum was most likely due to the combined effect of

high availability of CH_x adsorbed during the rich period and the transition through a surface O/Pt ratio with high activity. This indicates that the surface O/Pt ratio is crucial to the methane oxidation activity. An oxygen-rich surface seems to suppress the dissociative adsorption of methane, resulting in low methane oxidation activity at oxygen excess. The results suggest that in applications, transient operation (O_2 or H_2 pulsing) of the gas composition could be beneficial to maintain a surface composition favorable for high methane conversion. This is in line with previous observations for propane oxidation [33].

Acknowledgments

This work was supported by Swedish Research Council project 621-2005-3592 and the Competence Centre for Catalysis, which is hosted by Chalmers University of Technology and financially supported by the Swedish Energy Agency and the member companies AB Volvo, Volvo Car Corporation, Scania CV AB, GM Powertrain Sweden AB, Haldor Topsøe A/S, and the Swedish Space Agency. The authors thank the European Synchrotron Radiation Facility (ESRF), Grenoble, France, for providing the beamtime, and Dr. Mark Newton at beamline ID24 for assisting with the experiments.

References

[1] IPCC, Climate Change 2001, The Scientific Basis, Cambridge Univ. Press, London, 2001, p. 385, ch. 6.12.
[2] S. Oh, P. Mitchell, R. Siewert, J. Catal. 132 (1991) 287.
[3] R. Burch, P. Loader, Appl. Catal. B 5 (1994) 149.
[4] R. Burch, P. Loader, F. Urbano, Catal. Today 27 (1996) 243.
[5] R. Burch, D. Crittle, M. Hayes, Catal. Today 47 (1999) 229.
[6] P.-A. Carlsson, E. Fridell, M. Skoglundh, Catal. Lett. 115 (2007) 1.
[7] Y. Iwasawa, in: X-Ray Absorption Fine Structure for Catalysts and Surfaces, World Scientific, Singapore, 1996, p. V.
[8] B.M. Weckhuysen, *In situ* Spectroscopy of Catalysts, American Scientific Publishers, Stevenson Ranch, CA, 2004, p. 108.
[9] M. Englisch, J.A. Lerker, G.L. Haller, in: X-Ray Absorption Fine Structure for Catalysts and Surfaces, World Scientific, Singapore, 1996, p. 276.
[10] D. Koningsberger, B. Mojet, J. Miller, D. Ramaker, J. Synch. Rad. 6 (1999) 135.
[11] M. Teliska, W. O'Grady, D. Ramaker, J. Phys. Chem. B 108 (2004) 2333.
[12] T. Kubota, K. Asakura, Y. Iwasawa, Catal. Lett. 46 (1997) 141.
[13] Y. Yasawa, H. Yoshida, S. Komai, T. Hattori, Appl. Catal. A 233 (2002) 113.
[14] M. Brown, R. Peierls, E. Stern, Phys. Rev. 15 (1977) 738.
[15] J. Zhou, X. Zhou, X. Sun, R. Li, M. Murphy, Z. Ding, X. Sun, T.-S. Sham, Chem. Phys. Lett. 437 (2007) 229.
[16] J. Horsley, J. Chem. Phys. 76 (1982) 3.
[17] H. Yoshida, S. Nonoyama, Y. Yasawa, T. Hattori, Phys. Scr. T1115 (2005) 813.
[18] P.-A. Carlsson, L. Österlund, P. Thormählen, A. Palmqvist, E. Fridell, J. Jansson, M. Skoglundh, J. Catal. 226 (2004) 422.
[19] P. Lööf, B. Kasemo, S. Andersson, A. Frestad, J. Catal. 130 (1991) 181.
[20] S. Yoshida, T. Tanaka, in: X-Ray Absorption Fine Structure for Catalysts and Surfaces, World Scientific, Singapore, 1996, p. 309.
[21] M. Sanchez del Rio, R.J. Dejus, in: XOP: Recent Developments, in: SPIE-Int. Soc. Opt. Engin., vol. 2448, Bellingham, WA, 1998, p. 340.
[22] P. Hohenberg, W. Kohn, Phys. Rev. 136 (1964) 864.
[23] W. Kohn, L.J. Sham, Phys. Rev. A 140 (1965) A1133.
[24] M.C. Payne, M.P. Teter, D.C. Allan, T.A. Arias, J.D. Joannopoulos, Rev. Mod. Phys. 64 (1992) 1045.
[25] J.P. Perdew, K. Burke, M. Ernzerhof, Phys. Rev. Lett. 77 (1996) 3865.
[26] D. Vanderbilt, Phys. Rev. B 41 (1990) 7892.
[27] H.J. Monkhorst, J.D. Pack, Phys. Rev. B 13 (1976) 5188.
[28] J.D. Pack, H.J. Monkhorst, Phys. Rev. B 16 (1977) 1748.
[29] American Institute of Physics Handbook, McGraw–Hill, New York, 1979.
[30] M. Newton, A. Dent, S. Diaz-Moreno, S. Fiddy, B. Jyoti, J. Evans, Chem. Eur. J. 12 (2006) 1975.
[31] M. Newton, J. Synch. Rad. 14 (2007) 372.
[32] M. Ackermann, T. Pedersen, B. Hendriksen, O. Robach, S. Bobaru, I. Popa, C. Quiros, H. Kim, B. Hammer, S. Ferrer, J.W.M. Frenken, Phys. Rev. Lett. 95 (2005) 255505.
[33] P.-A. Carlsson, S. Mollner, K. Arnby, M. Skoglundh, Chem. Eng. Sci. 59 (2004) 4313.
[34] H. Yoshida, Y. Yasawa, T. Hattori, Catal. Today 87 (2003) 19.
[35] A. Bourane, D. Bianchi, J. Catal. 220 (2003) 3.
[36] J. Dicke, H. Rotermund, J. Lauterbach, Surf. Sci. 454–456 (2000) 352.
[37] R. Burwell, Adv. Catal. 26 (1977) 351.
[38] J. Ramallo-Lopez, F. Requejo, A. Craievich, J. Wei, M. Avalos-Borja, E. Iglesia, J. Mol. Catal. A 228 (2005) 299.
[39] A. Walker, B. Klötzer, D. King, J. Chem. Phys. 109 (1998) 6879.
[40] D. Watson, J. van Dijk, J. Harris, D. King, Surf. Sci. 506 (2002) 243.
[41] A.-P. Elg, F. Eisert, A. Rosén, Surf. Sci. 382 (1997) 57.
[42] K. DeWitt, L. Valadez, H. Abott, K. Kolanski, I. Harrison, J. Phys. Chem. B 110 (2006) 6705.
[43] J. Summers, K. Baron, J. Catal. 57 (1979) 380.